Published in final edited form as:

Nature. 2017 July 06; 547(7661): 114–117. doi:10.1038/nature22990.

RNase III nucleases from diverse kingdoms serve as antiviral effectors

Lauren C. Aguado[1,*], **Sonja Schmid**[1,*], **Jared May**[2], **Leah R. Sabin**[3], **Maryline Panis**[1], **Daniel Blanco-Melo**[1], **Jaehee V. Shim**[4], **David Sachs**[5], **Sara Cherry**[3], **Anne E. Simon**[2], **Jean-Pierre Levraud**[6], and **Benjamin R. tenOever**[1,**]

[1]Department of Microbiology, Icahn School of Medicine at Mount Sinai, New York, New York, 10029, USA

[2]Department of Cell Biology and Molecular Genetics, University of Maryland College Park, College Park, MD, 20742, USA

[3]Department of Microbiology, University of Pennsylvania, Philadelphia, PA 19104, USA

[4]Department of Pharmacology and Therapeutics, Icahn School of Medicine at Mount Sinai, New York, New York,10029, USA

[5]Department of Genetics and Genomic Sciences Icahn School of Medicine at Mount Sinai, New York, New York,10029, USA

[6]Macrophages et Développement de l'Immunité, Institut Pasteur and CNRS UMR3738, 25-28 rue du Dr. Roux, 75724 Paris Cedex 15. France

Abstract

In contrast to the DNA-based viruses in prokaryotes, the emergence of eukaryotes provided the necessary compartmentalization and membranous environment for RNA viruses to flourish, creating the need for an RNA-targeting antiviral system[1,2]. Present day eukaryotes employ at least two main defense strategies that emerged as a result of this viral shift, namely antiviral RNA interference (RNAi) and the interferon (IFN) system[2]. Here, we demonstrate that Drosha and related RNase III ribonucleases from all three domains of life, also elicit RNA-targeting antiviral activity. Systemic evolution of ligands by exponential enrichment (SELEX) on this class of proteins illustrates the recognition of unbranched RNA stem loops. Biochemical analyses reveal that in this context, Drosha functions as an antiviral clamp, conferring steric hindrance on the

**To whom correspondence should be addressed: Benjamin.tenOever@mssm.edu.
*Authors contributed equally

Author Contributions

LCA and SS designed and conducted experiments. MP performed SELEX. JM, LCA, and AES were responsible for plant data. LS and SC generated the *Drosophila* data. JVS generated the RNaseIII$^{-/-}$ cells. JPL and LCA performed the zebrafish work. DS and DBM were responsible for all bioinformatics. BRT, LCA, and SS wrote the paper.

Competing Financial Interests

The authors have no competing financial interests pertaining to this work.

Online Content

Methods, along with any additional Extended Data display items and Source Data, are available in the online version of the paper; references unique to these sections appear only in the online paper.

RNA dependent RNA polymerases (RdRps) of diverse positive stranded RNA viruses. We present evidence for cytoplasmic translocation of RNase III nucleases in response to virus in diverse eukaryotes including: plants, arthropods, invertebrate chordates, and fish. These data implicate RNase III recognition of viral RNA as an antiviral defense that is independent of, and possibly predates, other known eukaryotic antiviral systems.

MAIN

Life, as far back as self-replicating genetic material, demanded the capacity to generate and maintain sufficient diversity to allow for adaptation and evolution. In the approximately four billion years that followed, life and these self-replicating genetic entities co-evolved, creating an unremitting host-pathogen arms race[2]. From prokaryotic systems such as CRISPR to the RNAi systems of plants and invertebrates, many diverse antiviral strategies have proven successful in combating viral pathogens. As vertebrates transitioned from RNAi to IFN, remnants of this past system remain, including the two catalytically active RNase III members, Drosha and Dicer, both of which are critical for the biogenesis of microRNAs (miRNAs), a regulatory system designed on the same principles and machinery as antiviral RNAi[3].

As miRNA biology stemmed from the development of RNAi[4], but was not subjected to the selective pressures imposed by the biological arms race between host and pathogen, these components likely reflect the early eukaryotic RNAi machinery. This idea is supported computationally in model systems such as *Drosophila* where the antiviral Dicer (Dicer-2) underwent significant evolutionary changes as opposed to its miRNA counterpart (Dicer-1)[5]. Interestingly, of the two human RNase III nucleases, Drosha has greater homology than Dicer to the ancestral founder of this ancient domain[4]. The close relation of Drosha to its antiviral counterparts in invertebrates is particularly noteworthy given that this nuclease has recently been found to translocate to the cytoplasm following infection[6–8].

To better understand Drosha biology as it relates to the cellular response to virus infection, we disrupted the gene encoding Drosha in a previously characterized human Dicer-deficient cell line (NoDice cells) (Extended Data Fig. 1a)[9]. We characterized these cells (herein referred to as RNaseIII$^{-/-}$) cells by small RNA northern blot, probing for endogenous miR-93. As expected, mature miRNA levels in the parental NoDice cells could be restored by transfection of Dicer, whereas miR-93 expression in RNaseIII$^{-/-}$ cells required exogenous expression of both Dicer and Drosha (Fig. 1a). Small RNA sequencing from RNaseIII$^{-/-}$ cells confirmed a complete loss of all miRNAs both in the presence and absence of Sindbis virus (SINV) infection (Extended Data Fig. 1b).

SINV replication was dramatically elevated in RNaseIII$^{-/-}$ cells, as determined by the production and kinetics of capsid (SINV-C) protein (Fig. 1b). Specificity of this activity was assessed by infecting cells with positive vs. negative-stranded RNA viruses including: Ross River virus (Fig. 1c) and Langat virus (Fig. 1d), as well as Influenza A virus (Fig. 1e) and Sendai virus (Fig. 1f), respectively. These data demonstrated that only viruses of positive polarity had enhanced protein production in the absence of Drosha. Transcriptome profiling of NoDice and RNaseIII$^{-/-}$ cells at baseline revealed an induction of primary miRNAs and

DGCR8, a known target for Drosha-mediated cleavage[10,11] (Fig. 1g, Supplementary Table 1 and Extended Data Fig. 1c). Reconstitution of Drosha restored the transcriptome to that of NoDice cells (Extended Data Fig. 1d). In response to double stranded RNA (dsRNA), these cells showed little differential expression (Fig. 1h). Furthermore, we observed no defects relating to the IFN-I system (Extended Data Fig. 2a–2b). This phenotype was corroborated in primary *Rnasen*$^{f/f}$ conditional murine fibroblasts (Extended Data Fig. 2c–2e).

We next sought to identify the molecular basis for the impact of Drosha on positive-stranded RNA viruses. To ensure that Drosha's antiviral activity was not due to nuclear sequestration of a host RNA, we first generated a cell line expressing endogenous Drosha and GFP-Drosha S300A/S302A (herein referred to as Drosha-2A) which localizes exclusively to the cytoplasm (Extended Data Fig. 3a)[12]. Drosha-2A maintained enzymatic activity (Extended Data Fig. 3b) and, as predicted by our knockout studies, demonstrated an approximate one log decrease in SINV titers (Extended Data Fig. 3c). These data implicate cytoplasmic Drosha directly in the observed antiviral activity. Next, to map the domains required for this activity, we generated six deletion and/or site-specific Drosha mutants (Fig. 2a), all unable to process pri-miRNAs, including the catalytic mutant E1045Q/E1222Q[10] (herein referred to as RIIIDmut) (Fig. 2b). To test for antiviral activity of these mutants, we next exogenously expressed them together with replication-competent genomic SINV RNA. While Dicer exhibited no suppression of SINV, Drosha-WT efficiently reconstituted antiviral activity (Fig. 2c–d). This viral inhibition was also evident with a catalytically inactive RBmut that failed to associate with its canonical RNA binding partner, DGCR8 (Fig. 2e–2f).

RNase III nucleases are known to recognize RNA stem-loop structures in all three domains of life[13]. To identify RNA that associated with the RNase III domain of Drosha, we performed SELEX with RBmut. Five rounds of enrichment identified a subset of unique RNAs that lacked conserved sequences but folded into miRNA-like hairpin structures (Fig. 3a). GFP pull-downs yielded two dominant RNA species with complex predicted secondary structures that were evident in all samples, which were subsequently used as controls for specificity (Fig. 3b). Using a recombinant DroshaRB fragment, we corroborated specific association between Drosha's RNase III domain and an RNA hairpin identified by SELEX via electrophoretic mobility shift assay (EMSA), suggesting no other host factors were required for recognition of the RNA *in vitro* (Fig. 3c). These data were further corroborated using immunoprecipitated proteins from whole cell extract (Fig. 3d).

Given that the genomes of positive-stranded RNA viruses frequently utilize stem-loops similar to those identified by SELEX[14,15], we next investigated whether this RNase III domain could engage SINV RNA. In comparison to Flag-tagged SeV-NP, immunoprecipitated RBmut protein-RNA complexes in SINV-infected cells showed a one log enrichment of viral RNA (Extended Data Fig 4a–b). Moreover, RNA-EMSA confirmed RBmut interacted with a specific hairpin at the 5′ end of the genome (Extended Data Fig. 4c and d).

To better understand how Drosha engagement of these structures impedes replication we utilized a *Gaussia* luciferase-encoding Sindbis replicon system (Extended Data Fig. 5a). RNaseIII$^{-/-}$ cells produced significantly more genomic RNA, sub-gRNA, luciferase activity,

and antigenome compared to the NoDice parental cells (Fig. 3e–3g). These results suggest that Drosha is impacting RNA stability, translation, and/or directly blocking RdRp processivity. To assess the RNA stability hypothesis, we utilized a temperature-sensitive RdRp ($RdRp^{ts}$) SINV mutant that is inactive at 40 °C[16] (Extended Data Fig. 5b). At this nonpermissive temperature, no significant differences in genomic RNA decay in infected NoDice and $RNaseIII^{-/-}$ were observed (Extended Data Fig. 5c). To determine whether Drosha impacted translation, we measured the activity of a Firefly luciferase-encoding Sindbis construct *in vitro* ($SIN\text{-}nsP3^{Luc}$) and found Drosha presence to be inconsequential (Extended Data Fig. 5d–5e). Lastly, we assessed whether the RdRp itself was directly impeded. To this end, we utilized a Vaccinia virus-based system to generate functional minus strand-specific replicase complexes, as previously described[17]. Cellular fractions containing both SINV replicase and Drosha were isolated and assayed *in vitro*, demonstrating Drosha could reduce RdRp output by almost 50% (Fig. 3h and 3i).

As RNA hairpins, often essential for virus replication, are structurally conserved and evolutionarily constrained, they represent optimal targets for an antiviral system[18]. To determine if Drosha from other phyla can recognize this putative pathogen associated molecular pattern (PAMP) as demonstrated in both mammals and arthropods[19], we used miRNA-containing viruses to determine whether cytoplasmic processing, as an indicator of virus-induced translocation, could be observed. In zebrafish (*Danio rerio*), we demonstrated Drosha-dependent processing of a SINV-derived artificial microRNA in inoculated embryos (Fig. 4a and Extended Data Fig. 6a–6b). We next examined cytoplasmic processing activity in plants. To accomplish this, we cloned pri-miR-124 into *Turnip crinkle virus* (TCV) and infected *Arabidopsis* protoplasts cultures, which, like zebrafish, supported cytoplasmic miRNA processing (Fig. 4b and Extended Data Fig. 6c–6d).

Given the retention of this ancient activity, we turned to RNase III members from all domains of life (Extended Data Fig. 7a). Expression of each of these diverse nucleases, from bacteria, to archaea, to yeast, demonstrated robust antiviral activity against positive, but not negative, stranded viruses (Fig. 4c and 4d and Extended Data Fig. 7b). We next sought to demonstrate the antiviral activity of endogenous Drosha in an invertebrate. SINV-infected *D. melanogaster* cells were pretreated with dsRNA to knockdown Drosha as previously described[20]. Consistent with the results from mammalian cultures, loss of Drosha enhanced capsid expression (Extended Data Fig. 7c). Small RNA sequencing demonstrated that while more viral-derived RNAs were present in Drosha-depleted cells, the contour of mapped alignments were indistinguishable, ruling out a role for RNAi (Fig. 4e). This same phenotype was observed with Drosophila C virus (DCV) in *D. melanogaster*, and SINV in human cells (Fig. 4f and Extended Data Fig. 7d).

These results suggest that the RNase III family of nucleases, utilized in all domains of life for the maturation of ribosomal and other structural RNAs, may represent an ancient RNA recognition platform that helped eukaryotes combat viruses. Interestingly, of the two RNase III proteins encoded in the human genome, Drosha is more related to bacterial RNase III than is Dicer[4]. In contrast, Dicer has been suggested to be the ancestor that gave rise to MDA5 which later duplicated and generated RIG-I[21]. Given these evolutionary connections, it is tempting to speculate that the RNase III domain of prokaryotes may have provided an

early defense system for eukaryotes. In its most simple form, a Drosha-like homologue would recognize and engage RNA as an antiviral clamp but perhaps later evolve to utilize its enzymatic activity to give rise to RNAi. As the arms race continued, duplication, domain swapping, and time provided chordates the opportunity to use RNase III domains to create new RNA sensors and the eventual development of the IFN-I system which is believed to be fundamentally incompatible with RNAi[21–23]. As RNAi was functionally replaced with IFN-I during vertebrate development, the roles of Dicer and Drosha became largely dedicated to post transcriptional regulation. Despite all of the changes that have accrued over this expansive time, it iwould seem that fossils of this evolutionary arms race may remain in the basic biology of our miRNA machinery.

Methods

Viruses

Recombinant SINV, SINV124, and SINVamiRNA were previously described[7,24]. To generate SINV-GFP, the open reading frame of enhanced GFP was cloned under control of the additional subgenomic promoter of the SINV TE12Q construct[7,25], replacing miR-124. Virus infections in cell culture were performed using the specified MOI in DMEM without FBS for 1hr. Generation of a pre-miR-124 hairpin-encoding TCV was done as previously described[26]. Briefly, we inserted a gBlock (Integrated DNA Technology®) containing the 3′ end of the virus genome with the hairpin immediately downstream of the stop codon and flanked by BssHII and MluI into the MscI and SpeI sites of the pTCV66 construct. A control sequence was subsequently inserted by replacing miR-124 in the BssHII and MluI sites. A/Puerto Rico/8/34 (H1N1) Influenza virus (IAV) was rescued as previously described[27]. Ross River Virus, strain T-48, was purchased from ATCC (VR-373) and amplified on BHK21 cells. Langat (strain TP21) and Sendai-GFP viruses were kind gifts from Drs. Jean Lim and Benhur Lee (Icahn School of Medicine at Mount Sinai, NY), respectively. Vaccinia viruses encoding T7 DNA-dependent RNA polymerase, ubiquitin-tagged SINV nsP4, and the SINV polyprotein $123_{C>S,}$ containing a mutation rendering nsP2 protease activity nonfunctional, were kind gifts from Dr. Richard W. Hardy (Indiana University, Bloomington, IN). Adenoviruses expressing GFP or Cre were purchased from Vector Biolabs (Cat# 1768 and 1779).

Cell culture and reagents

Drosophila cells (DL1) were grown, maintained and treated with dsRNA as previously described[20,28]. All mammalian cells were cultured in DMEM supplemented with 10% FBS and 1x penicillin/streptomycin (pen/strep). HEK 293T (293T) cells were purchased from ATCC (CRL-3216). NoDice 293T cells were a kind gift from Dr. Bryan R. Cullen (Duke University, Durham, NC)[9]. BSR-T7 cells were generously provided by Dr. Karl-Klaus Conzelmann (Ludwig-Maximilians-University, Munich). $Rnasen^{f/f}$ primary lung fibroblasts were a kind gift from Dr. Dan Littman (New York University) and are described elsewhere[29]. 293T cells stably expressing GFP-tagged Drosha-WT or Drosha-2A were generated using a lentiviral expression vector and selected with puromycin (1μg/ml). To generate $RNaseIII^{-/-}$ cells, the CRISPR/Cas9 system was utilized to disrupt Drosha in NoDice cells. A custom made plasmid encoding for two guide RNAs targeting the human

RNASEN gene, nickase Cas9, and GFP (NickaseNinja) were purchased from DNA2.0. NoDice cells were transfected with this plasmid and GFP expressing cells were single-cell sorted into 96-well plates. To identify clones lacking a functional Drosha protein, we PCR amplified and sequence verified the targeted genomic region. Co-transfection of plasmids and SINV *in vitro* transcribed genomic RNA was performed using Lipofectamine 2000 (Thermo Fisher®) as per the manufacturer's instructions. In brief, 1.75×10^6 cells were transfected using 4 μg of plasmid DNA, 0.5 μg of RNA and 6 μl of transfection reagent. Transfection with *in vitro* transcribed SINV minigenome RNA was performed using Transmessenger Reagent (Qiagen®) as per the manufacturer's instructions. In brief, 1.5×10^5 cells were transfected with 0.8 μg RNA and 4 μl transfection reagent. All cell lines used in these studies were routinely screened for mycoplasma.

Plasmids

The CMV promoter driven Langat virus rescue plasmid was a kind gift from Dr. Alexander G. Pletnev (National Institute of Allergy and Infectious Diseases)[15]. Sendai virus rescue plasmids encoding the SeV-GFP genome, SeV-N, SeV-P, and SeV-L were a kind gift from Dr. Benhur Lee (Icahn School of Medicine at Mount Sinai, NY). The pMini(+) SINV minigenome plasmid was a kind gift from Dr. Richard W. Hardy (Indiana University, Bloomington, IN)[17]. GFP-tagged Drosha mutants were generated starting from pEGFP-Drosha-WT[12]. The two point mutations in the RIIIDs (E1045Q/E1222Q) were introduced by site-directed mutagenesis. To generate GFP-tagged deletion mutants, the desired fragment of Drosha was PCR amplified and cloned into pEGFP-Drosha-WT using the In-Fusion HD Cloning Kit (Clontech®). GFP-tagged *Ciona intestinalis* and *Streptococcus pyogenes* constructs were generated using synthesized gBlock fragments of the C-terminal 425 amino acids of *C. intestinalis* or full length *S. pombe* Pac1, and *M. maripaludis* or *S. pyogenes* RNase IIIs into the HindIII and KpnI sites of pEGFP-C1. A construct containing two tandem codon optimized FAK NES2[30] sequences was additionally inserted into the HindIII site of the pEGFP-*C.intestinalis*-Drosha construct using the In-Fusion HD Cloning Kit (Clontech®). To generate a plasmid encoding for the SINV replicon expressing *Gaussia* luciferase, we PCR amplified the open reading frame of *Gaussia* luciferase and cloned it into the SINV TE12Q construct[25] via NarI and ApaI using the In-Fusion HD Cloning Kit (Clontech®). The resulting SINV replicon encodes for *Gaussia* luciferase fused to 76 nts of the SINV capsid protein. To generate SINV expressing a temperature sensitive RdRp (SIN-RdRp^{ts}), we substituted glycine 153 of non-structural protein four (ns4) to glutamic acid as previously described[16]. G153E was generated using a synthesized gBlock fragment cloned into SpeI and HpaI of the SINV TE12Q construct[26]. Luciferase reporter constructs for translational inhibition were generated by inserting sequences into the HindIII and EcoRI sites upstream of *Gaussia* luciferase in the pcDNA-Gluc-polyA construct. Scrambled, pre-mmu-miR-124-2, Ctrl-1, and HP-2 sequences were mutated to remove internal ATGs, synthesized as gBlock fragments, and inserted using the In-Fusion HD Cloning Kit (Clontech®).

Northern blot analysis

Total RNA was isolated using Trizol (Thermo Fisher®) as per the manufacturer's instructions. Small RNA northern blotting was performed as previously described[27,31]. For

large RNA northern analysis, 5 μg of total RNA in loading buffer (30% (v/v) formamide, 3% (v/v) formaldehyde, 5% (v/v) glycerol, 1x MOPS, and 0.01% (w/v) bromophenol blue) was separated in a 1% agarose gel in 1x MOPS buffer. RNA was transferred by capillary action in 20x SSC buffer (3 M NaCl, 0.3 M sodium citrate, pH 7.0) onto Hybond-NX nylon membrane (GE Healthcare). RNA was then UV cross-linked to the membrane (0.2 mJ/cm^2) and incubated in blocking buffer (6x SSC and 7% SDS) for 1hr at 65 °C. Next, the membrane was incubated with a radio-labeled DNA oligonucleotide overnight at 42 °C in 6x SSC and 7% SDS, washed three times for 10min in 3x SSC and 0.1% SDS, and exposed to film. Sequences of probes are listed in Supplementary Table 2.

Quantitative PCR (qPCR)

Total RNA was isolated with Trizol (Thermo Fisher) and reversed transcribed using SuperScript II (Thermo Fisher®) as per the manufacturer's instructions. cDNA was amplified with gene specific primers using a KAPA SYBR green master mix (KAPA Biosystems®) and analyzed on a LightCycler 480 (Roche®). Sequences of gene-specific primers are listed in Supplementary Table 2.

RNA sequencing

For mRNA-Seq, libraries from two biological replicates per condition were prepared with the TruSeq RNA Library Preparation Kit v2 (Illumina®) as per the manufacturer's instructions. In brief, 1 μg of total RNA was enriched for mRNA using oligo-dT beads. Purified RNA was fragmented and reverse transcribed, followed by second-strand synthesis, end repair, A-tailing, adapter ligation, and PCR amplification. Prepared libraries were then quantified using the universal complete KAPA Library Quantification Kit (KAPA Biosystems®). Libraries were sequenced on an Illumina MiSeq platform with the MiSeq Reagent Kit v3 or on a HiSeq 2500. Sequence reads were analyzed with the RNA Express application (Illumina, BaseSpace) or custom pipelines. Alignment of reads to viral genomes was performed using Bowtie and subsequently visualized using the Integrative Genomics Viewer[32] (citation). The correlation analyses were performed by comparing the natural logarithm of the normalized read counts (reads per million) between two experimental settings. The Pearson correlation coefficient (r) was calculated using the cor() function in R with default parameters. For each experimental setting the average normalized read count was calculated first using two biological replicates. Small RNA sequencing of infected DL1 cells was performed as previously described [20]. Briefly, cells were treated with indicated dsRNA for 3 days and subsequently infected with SINV (MOI=1) or DCV (MOI=7) for 96 hrs before RNA extraction. Total RNA (40 ug) was separated on a 15% TBE-urea gel. The ~15–29 nt fraction was extracted, eluted, and ethanol precipitated. Libraries were prepared using the Small RNA Sample Prep v1.5 kit (Illumina, San Diego, CA) as per manufacturer's instructions and sequenced on an Illumina Genome Analyzer II. Libraries for small RNA sequencing of 293T and RNaseIII$^{-/-}$ cells were prepared using 1ug of total RNA and the Small RNA Sample Prep v1.5 kit (Illumina, San Diego, CA) as per manufacturer's instructions. The entire small RNA fractions (~15–200 nt) were gel extracted and barcoded samples were PCR amplified for an additional 25 cycles before sequencing on an Illumina MiSeq platform with the MiSeq Reagent Kit v3. Adapters were trimmed and analysis was performed using the Small RNA Sequencing App from Illumina. Raw and processed data

can be found on NCBI's Gene Expression Omnibus (GEO) using accession numbers GSE86610, GSE89790, GSE96889, GSE43031, and GSE98135.

Antiviral assays

RNaseIII$^{-/-}$ cells were co-transfected with Drosha, Drosha variants, or RNase III plasmids and either *in vitro* transcribed SINV RNA, Langat rescue plasmid. At 24 hpt for SINV, 30 hpt for Langat, cells were harvested and virus replication was assessed by Western blot. BSR-T7 cells were co-transfected with indicated RNase III constructs and a pool of Sendai virus rescue plasmids (described above). BSR-T7 samples were harvested at 48 hpt for assessment of RNase III expression and at 72 hpt for virus replication.

Immunoprecipitations

For immunoprecipitations of Flag-GFP and –DGCR8, 2 × 10^6 293T cells were transfected with 2 μg each of the indicated plasmids. At 24 hpt, cells were lysed in 50 mM Tris pH=7.5, 10% glycerol, 1mM EDTA, 30 mM NaF, 1% NP-40, 150 mM NaCl, 1x PMSF, and 1 × protease inhibitor cocktail and sonicated 1x for 15 seconds. Lysates were rotated overnight at 4 °C with 5μl anti-Flag M2 antibody before addition of 25 μL protein G agarose beads. Samples were rotated for 1.5 hrs, washed in the same buffer used for lysis. and then analyzed by western blot.

RNA immunoprecipitation was performed as previously described[33]. Briefly, 36 hpt of RNaseIII$^{-/-}$ cells with the indicated plasmids, cells were infected with SINV at an MOI of 3. At 7 hpi, cell lysates were prepared in lysis buffer (15 mM Tris/HCl pH 7.5, 150 mM NaCl, 15 mM $MgCl_2$, and 1% (v/v) TritonX-100) supplemented with 10 mM of Ribonucleoside Vanadyl complex (NEB S1402S) and 1x protease inhibitor cocktail (Roche). Cell lysates were incubated with anti-Flag affinity resin (Sigma A2220) at 4 °C for 2 hrs followed by four washes 5 min each with lysis buffer. Protein-RNA complexes were eluted with 300 μg/ml Flag-peptide (Sigma F3290) and purified RNA was extracted using Trizol.

Systematic evolution of ligands by exponential enrichment (SELEX)

SELEX was performed as previously described[34]. Briefly, a T7 promoter-driven library of 92,918 scrambled 110mer oligos was synthesized by CustomArray Inc®. The DNA oligo library was PCR amplified, followed by *in vitro* transcription using the MEGAscript T7 Transcription Kit (Thermo Fisher®) as per the manufacturer's instructions. RNA was heated at 65°C for 5 min and immediately put on ice before the selection process. Flag-tagged proteins were purified from RNaseIII$^{-/-}$ cells at 24 hpt in lysis buffer (15 mM Tris/HCl pH 7.5, 150 mM NaCl, 15 mM $MgCl_2$, and 1% (v/v) TritonX-100) supplemented with 1x protease inhibitor cocktail (Roche®). Cell lysates were incubated with anti-Flag affinity resin (Sigma A2220) at 4 °C overnight, followed by four washes 5 min each with lysis buffer. 1 μg of *in vitro* transcribed RNA in lysis buffer was added to the beads and incubated at 4 °C for 2 hrs, followed by four washes 5 min each with lysis buffer. Protein-RNA complexes were eluted with 300 μg/ml Flag-peptide (Sigma F3290) and purified RNA was extracted using Trizol. Purified RNA was reverse transcribed, PCR amplified and *in vitro* transcribed to repeat the selection process. A total of 5 rounds of selection were performed.

Electrophoretic mobility shift assay (EMSA)

EMSAs were performed as previously described[35]. Flag-tagged proteins were purified from RNaseIII$^{-/-}$ cells at 24 hpt in lysis buffer (15 mM Tris/HCl pH 7.5, 150 mM NaCl, 15 mM $MgCl_2$, and 1% (v/v) TritonX-100) supplemented with 1x protease inhibitor cocktail (Roche®). Cell lysates were incubated with anti-Flag affinity resin (Sigma A2220) at 4 °C overnight, followed by four washes at 5 min each with lysis buffer. Bound protein was eluted with 300 μg/ml Flag-peptide (Sigma F3290) in 20 mM Tris/HCl pH 8.0, 100 mM KCl, and 0.2 mM EDTA. Alternatively, a fragment of recombinant human Drosha protein was purchased from Abcam (ab94010) and 0.25–1 μg of this purified protein was used for EMSAs. Radioactively labeled RNA was *in vitro* transcribed from a PCR-amplified template using the MAXIscript kit (Ambion®). For complex formation of protein and RNA, protein eluate or recombinant protein was incubated with radio-labeled RNA (~100,000 cpm per reaction) for 30 min at room temperature in 20 mM Tris/HCl pH 8.0, 100 mM KCl, and 0.2 mM EDTA, supplemented with 0.1 μg/μl BSA and 1 mM DTT. Reactions were run on a 6% polyacrylamide gel.

In vitro cleavage assay

In vitro cleavage assays with Drosha were performed as previously described[36].

in vitro minus strand RNA synthesis assay

in vitro minus strand assays were performed as previously described[37]. Briefly, 293T or 293T Drosha-2A cells were infected for 6 hrs with VacV-T7, -nsP4-ub, and - nsP123$_{C>S}$ at an MOI=5 for each virus. Cells were resuspended in hypotonic buffer (10 mM Tris-HCl [pH 7.4] and 10 mM NaCl) and allowed to swell on ice for 15 min then lysed by 50 strokes through a 25 G 5/8 needle. Nuclei were removed by centrifugation (900 g for 5 min at 4 °C). Membranes were isolated from the remaining supernatant by centrifugation at 15,000 g for 20 min at 4 °C. Pellets were resuspended in hypotonic buffer plus 15% glycerol, aliquoted, and stored at −80 °C. Reactions were performed in a total volume of 50 μL in a mixture containing 50 mM Tris-HCl [pH7.4], 50 mM KCl, 3.5 mM $MgCl_2$, 10 mM DTT, 10 μg actinomycin D per mL, 1 mM each ATP, GTP, and UTP, 40 μM CTP, 1 μL CTP, [α-32P]-800Ci/mmol 10mCi/ml EasyTide, 250 μCi per reaction, 1 μL RNaseOUT (Thermo Fisher, 10777019), 0.8 μg pMini(+) *in vitro* transcribed RNA template, approximately 25 μg (total protein input adjusted to ensure equal nsP4 levels across cell types, quantified from western blots using ImageJ software) membrane fractions, and H_2O for 1.5 hrs at 30 °C before 5 U of alkaline phosphatase was added and the incubation continued for another 20 min. The reactions were terminated by the addition of SDS to 2.5% and proteinase K at a final concentration of 100 μg/mL. RNA was isolated with TRIzol, equal volumes were run on a 1.25% agarose gel, transferred onto Hybond-NX nylon membrane (GE Healthcare) and exposed to film.

in vitro translation assay

In vitro translation assays were performed using the Rabbit Reticulocyte Lysate System (Promega) according to the manufacture's instructions. Membrane fractions (10 μg) from uninfected 293T and 293T Drosha-2A cells and 2 μg of SINV-nsP3^{Luc} RNA were added to

the reaction components, incubated for 2 hrs at 30 °C before analysis for Firefly luciferase production.

Western blot analysis

Whole cell extracts were separated on Mini Protean TGX gels and transferred onto nitrocellulose membrane (BioRad®). SINV-specific ascites fluid (ATCC-VR-1248AF) and antibodies specific to actin (Thermo Fisher®, MS-1295-P), GAPDH (Sigma®, G9545), Flag (Sigma®, F1804), NS1 (CTAD, Icahn School of Medicine at Mount Sinai), STAT1a (Santa Cruz, c-111), and RIG-I (Generously provided by Dr. Adolfo Garcia-Sastre, Icahn School of Medicine at Mount Sinai, NY) were used at a dilution of 1:1000 in 5% milk. Russian spring-summer encephalitis virus ascites fluid (ATCC- V558701562) was used for the detection of Langat virus at a dilution of 1:500 in 5% milk. Antibodies specific to GFP (Santa Cruz, sc-8334) and RRV-specific ascites fluid (ATCC-VR-1246AF) were used at a dilution of 1:200 in 5% milk. The SINV nsP4 antibody was a kind gift from Dr. Richard W. Hardy (Indiana University, Bloomington, IN) and was used at a 1:5,000 dilution in 5% milk in 25 mM Tris-HCl [pH 7.4], 137 mM NaCl, 2.7 mM KCl. and 0.1% Tween20. Mouse and rabbit HRP-conjugated secondary antibodies (GE Healthcare®) were used at a 1:2000 dilution in 5% milk. For antibody detection, Immobilon Western Chemoluminescent HRP (Millipore®) and SuperSignal™ West Femto Maximum Sensitivity (Thermo Fisher®) substrates were used according to the manufacture's instructions.

Luciferase assays

For assessment of translational inhibition by Drosha viral RNA binding, SINV replicon constructs (described above) were in vitro transcribed using an SP6 mMessage Machine Kit (Ambion®) and co-transfected with a control Gaussia luciferase RNA as described for hairpin constructs. Luciferase expression was analyzed at indicated time points post-transfection using the Promega Dual-Luciferase® Reporter Assay System. In all experiments, *Gaussia* luciferase expression was normalized to Firefly luciferase.

in vivo infections

Zebrafish embryos (AB strain) were randomly pooled in groups and injected with 8 ng of control (GAAAGCATGGCATCTGGATCATCGA) or of Drosha translation blocking (AGTGAAACTGAAGCAAACCTGTCCA) morpholinos at the 1-cell stage (sex was not determined). At 2 days post-fertilization, embryos were inoculated intravenously and intracranially, receiving a total of ~5000 pfu of SINVwt or SINVamiRNA. RNA was extracted from surviving larvae at 40 hrs post infection. Each sample is a pool of 5–11 larvae. Zebrafish experiments were performed in accordance with the Institute Pasteur Animal Care and Use Committee (CEEA 89).

Protoplasts were prepared from callus cultures of *Arabidopsis thaliana* (Col-0-strain). Transfections were performed using polyethylene-glycol as previously described[38]. Briefly, 15 μg of T7-transcribed TCV genomic RNA was transfected into 7×10^6 cells in a 60 mm petri dish and incubated in the dark at 22 °C for 40 hrs. Samples were collected at 13,000 rpm. Total RNA was isolated using RNA extraction buffer (50 mM Tris-HCl pH 7.5, 5 mM

EDTA pH 8.0, 100 mM NaCl, 1% SDS), followed by phenol-chloroform extraction and ethanol precipitation.

Fluorescence *in situ* hybridization

Fluorescence *in situ* hybridization of *Arabidopsis thaliana* protoplasts (FISH) was performed following an established protocol[39]. Briefly, mock and TCV-infected protoplasts were fixed with methanol and hybridized with 4 μM Cy3-labelled probe complementary to bases 1210–1259 of the TCV genome (5′-Cy3-GCCTTCACGAATGTTTTGAGTTCTGCGTCCTTCCGGGATACCGGTCTGTC-3′). Cells were collected and washed with 2X SSC + 10% formamide before mounting with ProLong Gold + DAPI (Invitrogen). Cells were imaged using a laser scanning LSM 710 AxioObserver confocal microscope (Carl Zeiss). Images were acquired using a 63x/1.40 Oil DIC objective with 405 nm and 561 nm filters for DAPI and Cy3 respectively.

Zebrafish larvae were infected as described above and fixed at 24 hrs post-infection. Whole-mount FISH was performed using a FITC-labeled SINV capsid probe amplified with anti-FITC-AF488. Hoechst dye was used for detection of nuclei. Single confocal plains from an infected region in the tail were imaged using a 40x objective.

Data availability

Deep sequencing data has been deposited in the Gene Expression Omnibus under accession numbers GSE86610, GSE89790, GSE96889, GSE43031, and GSE98135. All other data available from the corresponding author upon reasonable request.

Extended Data

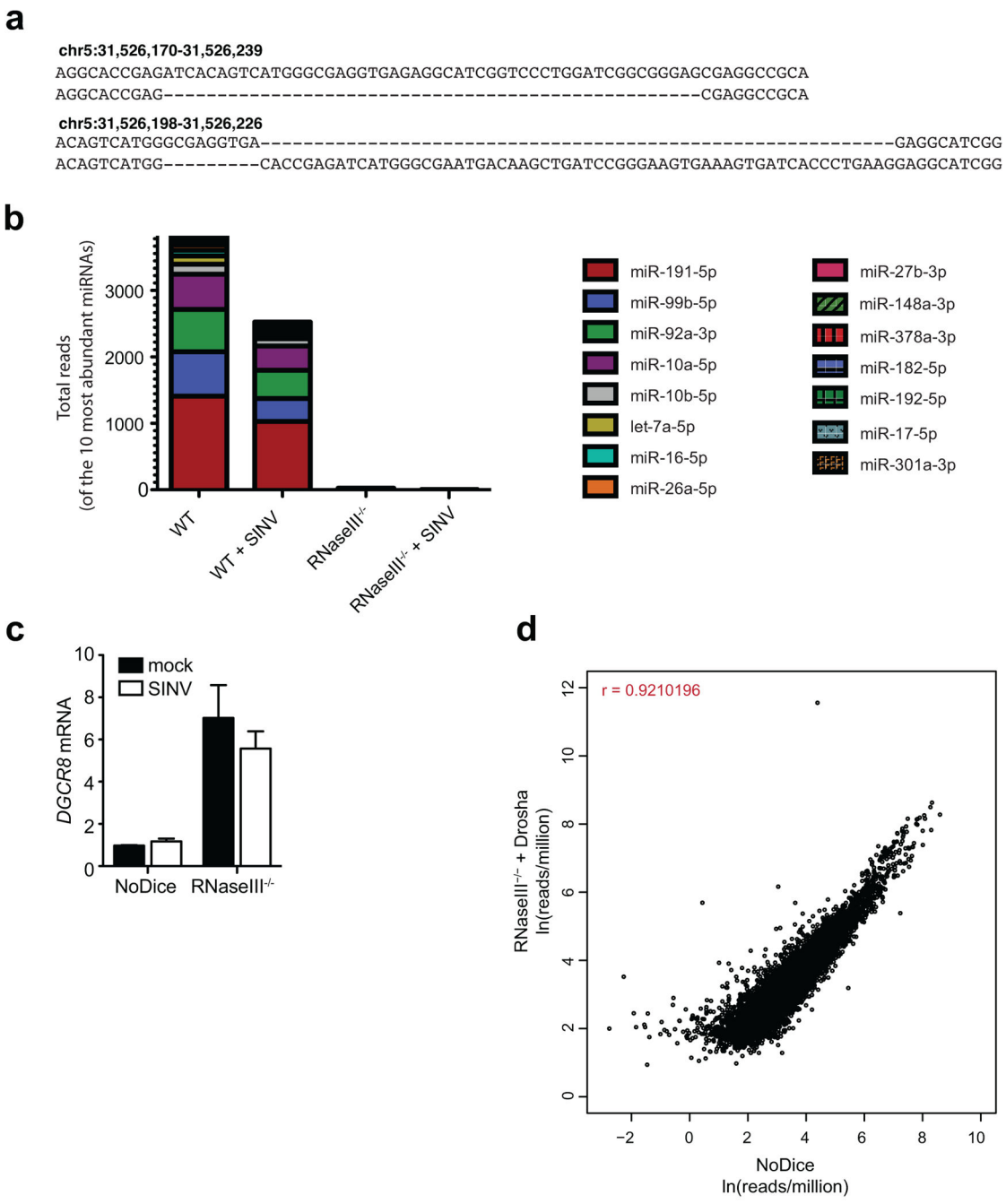

Extended Data Figure 1. Characterization of RNaseIII$^{-/-}$ cells

a, Sequence alignment of genetic alterations in the two alleles encoding Drosha in RNaseIII −/− cells. The deletion and insertion result in a frameshift and early stop codon. b, Graph depicts the ten most abundant miRNAs in each condition, parental 293T (WT) or RNase III −/− either mock or SINV-infected for 24 hrs as determined by Illumina small RNA deep sequencing. c, qPCR analysis of DGCR8 mRNA levels in mock treated and SINV-infected

(MOI=0.1, 8hpi) NoDice and RNaseIII$^{-/-}$ cells. d, Transcriptome profiling and correlation analyses of NoDice cells at baseline and RNaseIII$^{-/-}$ cells transfected with GFP-tagged human Drosha for 72 hrs. Graph depicts data from two biological replicates per condition.

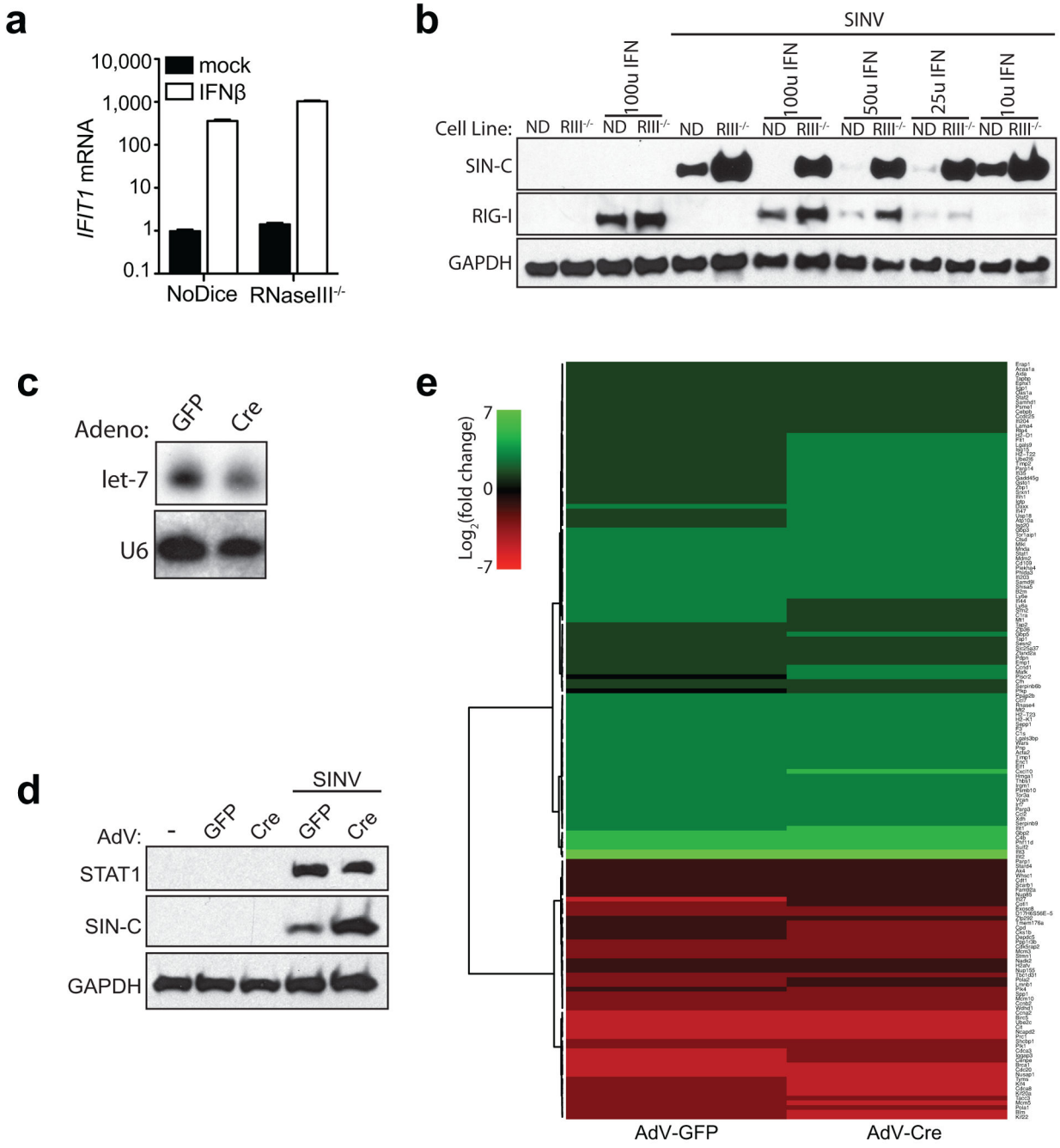

Extended Data Figure 2. Drosha depletion does not alter the response to IFN-I

a, qPCR analysis of IFIT1 mRNA levels in NoDice and RNaseIII$^{-/-}$ fibroblasts treated with IFNβ (100 u/ml, 8 hrs). b, Western blot of NoDice and RNaseIII$^{-/-}$ fibroblasts infected with SINV for 1 hr prior to administration of indicated amounts of IFNβ for 24 hrs. c–e, Northern

blot (c) and western blot (d) of primary Rnasenf/f ear-derived fibroblasts treated with indicated AdVs for 2–3 days and then treated with either 100U IFNβ for 6 hrs (b) or infected with SINV for 24 hrs (d). e, mRNA-Seq of total RNA from samples in (c). Heatmap depicts known mouse ISGs and IFN down regulated genes with a log2 fold change greater than 1, as defined by the Interferome database (www.interferome.org).

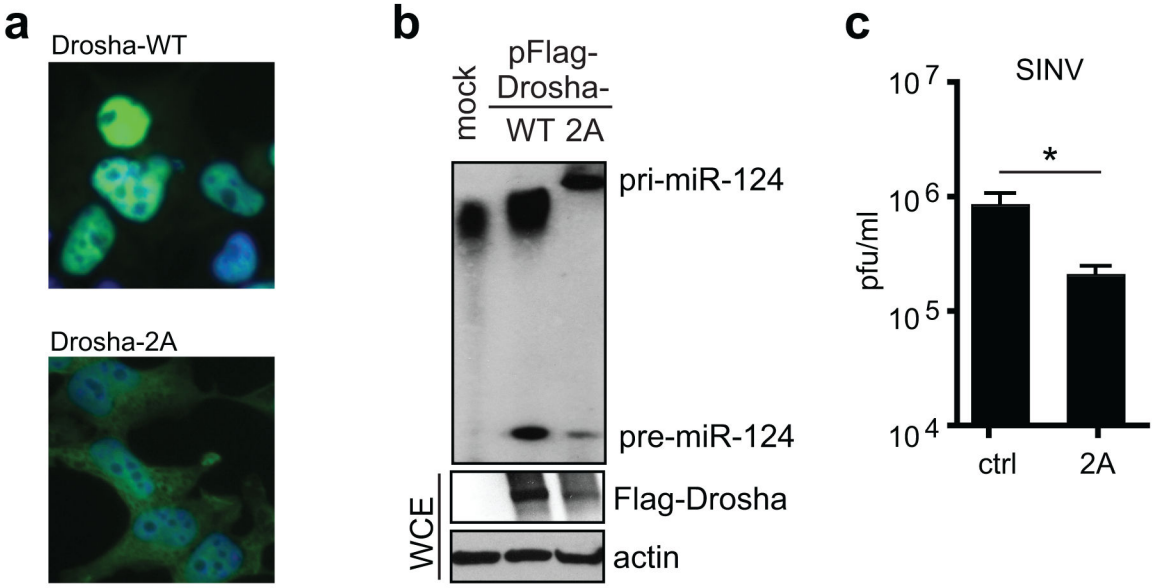

Extended Data Figure 3. Characterization of Drosha-2A cells

a, Immunofluorescence of human fibroblasts stably expressing GFP-tagged Drosha-WT or Drosha-2A (S300A/S302A). b, The indicated Flag-tagged proteins were immunoprecipitated from whole cell extracts (WCE) and incubated at 37 °C with in vitro transcribed genome of SIN124. Production of pre-miR-124 was determined by small RNA northern blot. c, Indicated cell types were infected with SINV at an MOI of 0.001 and viral titers were determined at 16 hpi. Shown is average and standard deviation of three independent experiments, with $p<0.05$ as determined using a two-tailed student's t-test.

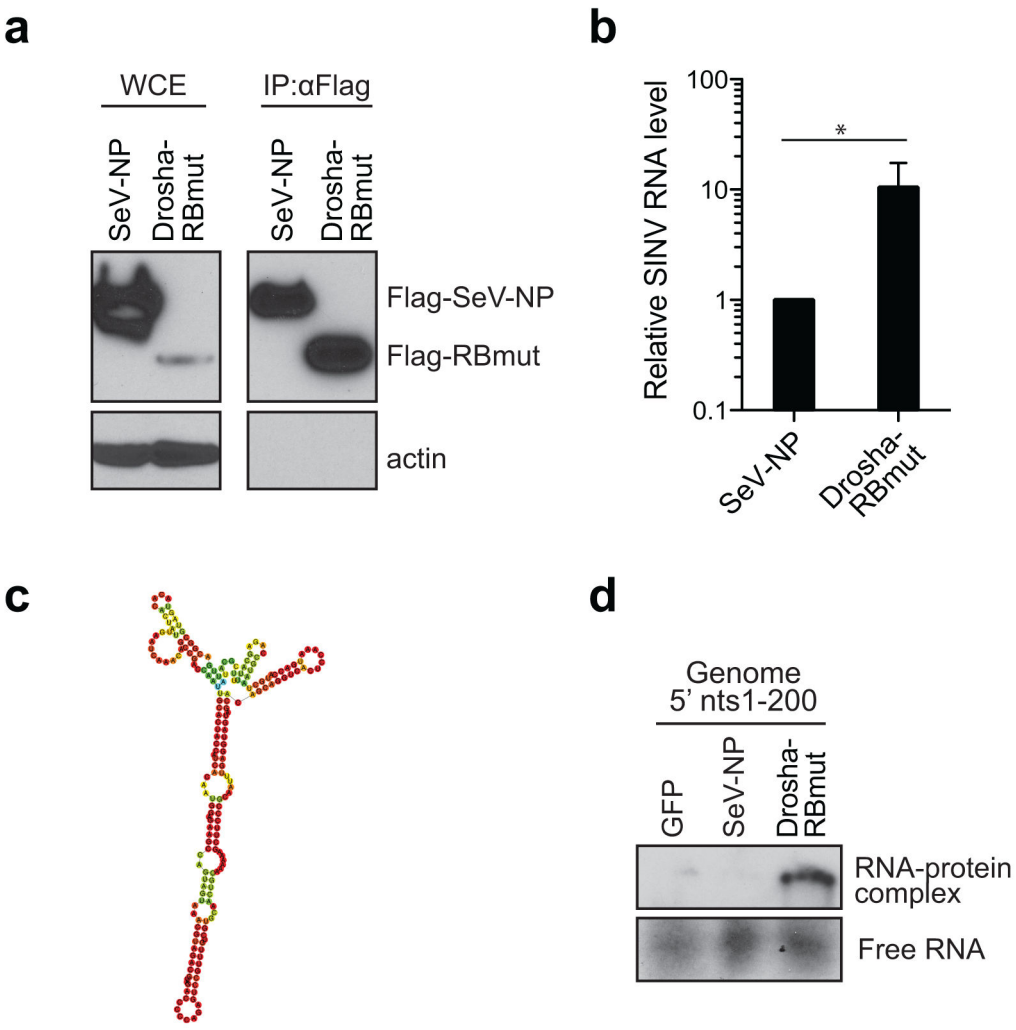

Extended Data Figure 4. Drosha-RB-RIIIDmut recognizes stem-loop structures in SINV RNA

a, Immunoprecipitation of exogenously expressed Flag-tagged proteins. Shown is protein expression in the whole cell extract (WCE) and after immunoprecipitation (IP) with a Flag-specific antibody. **b**, Cells were transfected with Flag-tagged SeV-N or Drosha-RBmut and infected at 36 hpt with SINV at an MOI of 3. 8 hpi, Flag-tagged proteins were immunoprecipitated and bound RNA was isolated to perform qPCR. Graph shows SINV RNA levels relative to input and normalized to tubulin. The average of three independent experiments is shown. Error bars depict standard deviation and * denotes $p<0.05$ using a one-tailed student's t-test. **c**, Prediction of the structure of the 5′ 200 nts of the SINV genome using RNAfold. **d**, EMSA was performed with the indicated immunoprecipitated proteins and radio-labeled in vitro transcribed RNA comprising the 5′ 200 nts of the SINV genome. Unbound genome is indicated as 'Free RNA'.

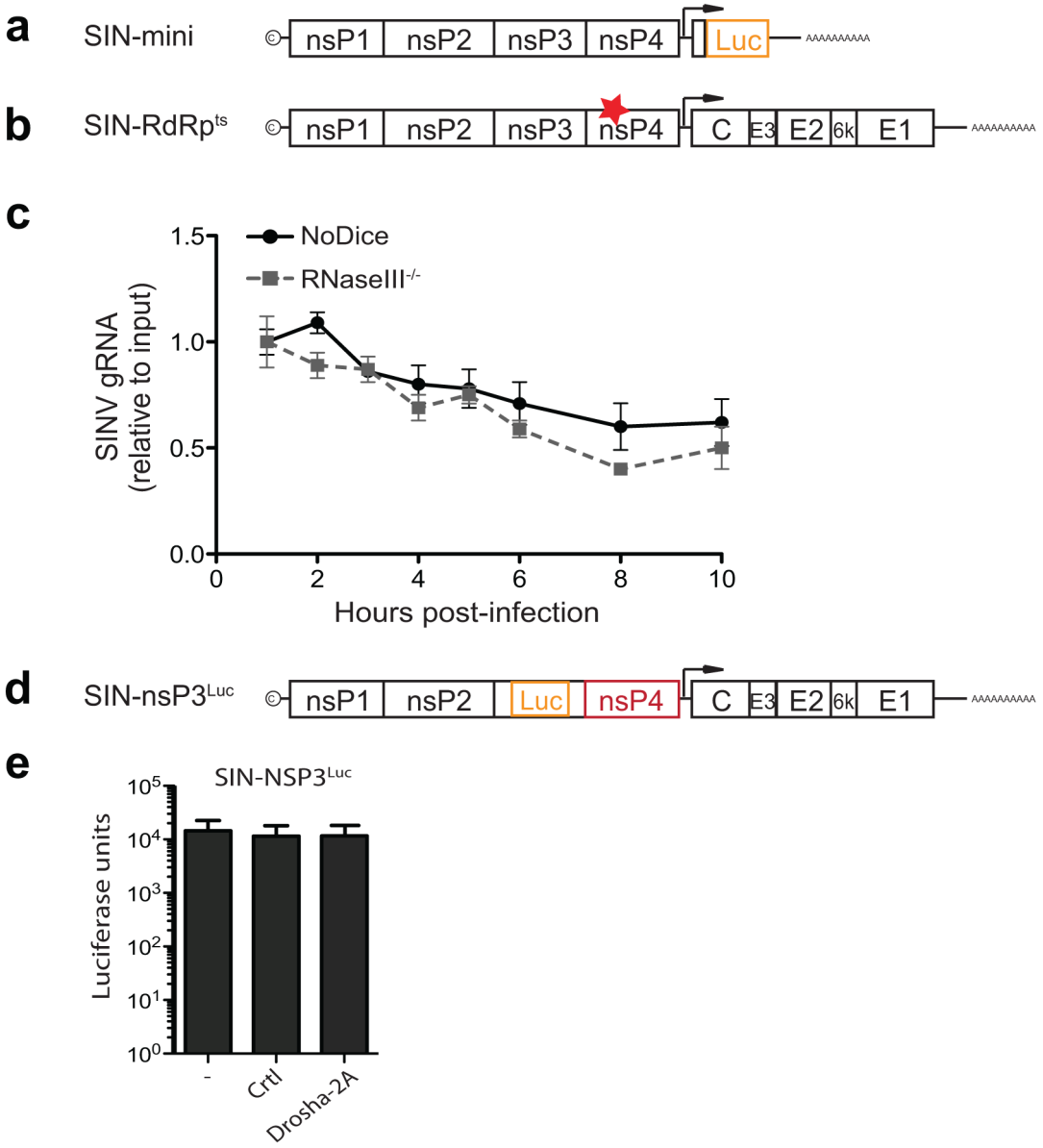

Extended Data Figure 5. Using virus engineering to discern Drosha's antiviral mechanism

a, Schematic of the SINV replicon encoding Gaussia luciferase in place of the structural polyprotein used in Figs. 3e–g. b, Schematic of the SINV temperature sensitive mutant (SIN-RdRpts). Star denotes ts point mutant. **c**, NoDice and RNaseIII$^{-/-}$ cells were infected with virus depicted in **b**, at an MOI of 10 and incubated at 40 °C, a temperature at which the mutant viral RdRp is completely inactive. Levels of genomic (g) SINV RNA were determined by qPCR at indicated times post infection. Data is representative of two independent experiments where each condition was done in triplicate. **d**, Schematic of the SINV encoding Firefly luciferase in the nsP3 region and an inactive RdRp (SIN-nsP3Luc) **e**, Graph depicts levels of in vitro translation of Firefly luciferase produced from virus in d, in the presence of membrane fractions from control or Drosha-2A. The data shown is the average of three independent experiments.

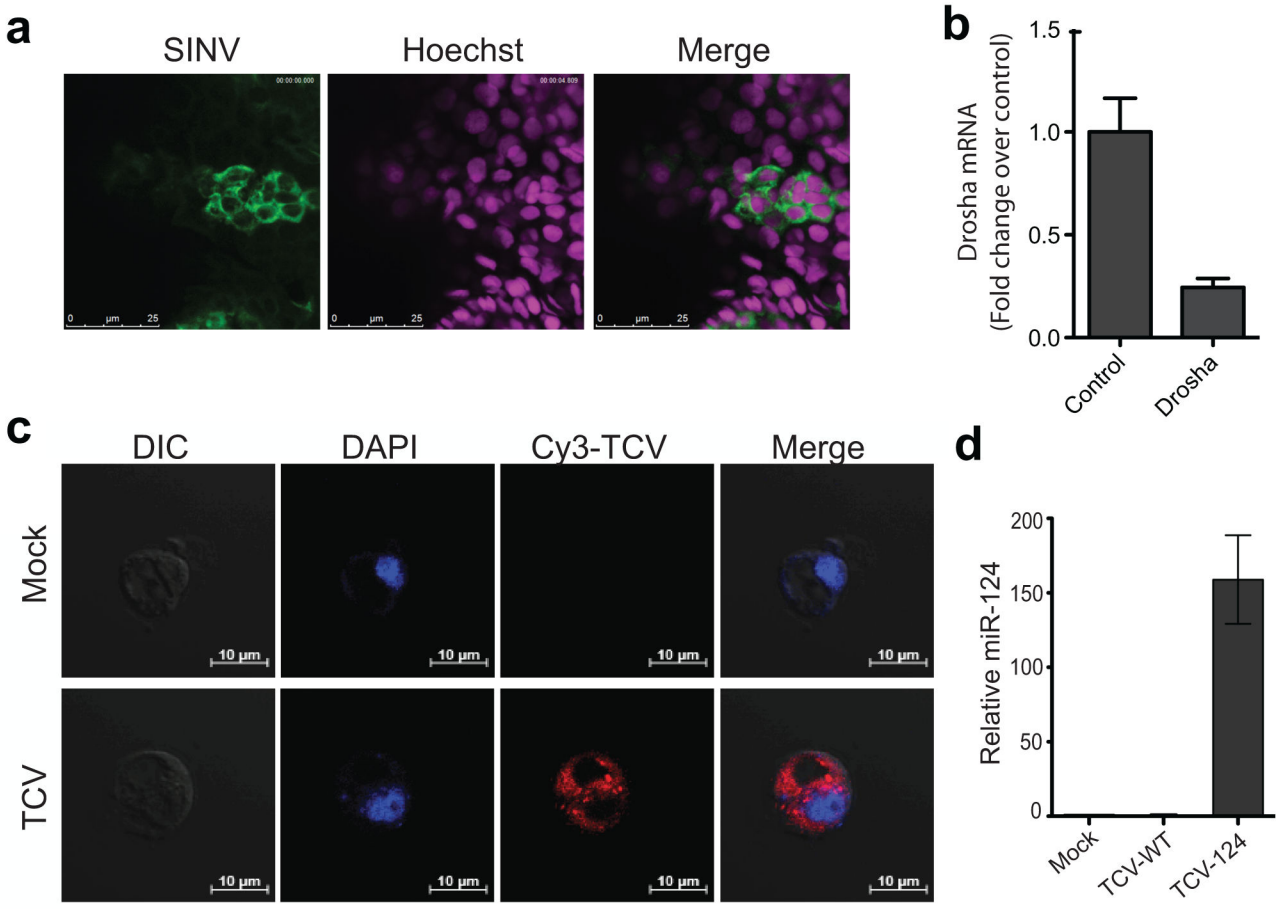

Extended Data Figure 6. Localization of and miRNA production from cytoplasmic viruses in diverse eukaryotes

a, Zebrafish embryos were inoculated with SINV for 24 hrs and then analyzed by fluorescence in situ hybridization (FISH) using a probe complementary to the capsid region of the genome. **b,** qPCR analysis of zebrafish embryos treated with indicated morpholinos for 2 days (n=4). **c**, *Arabidopsis thaliana* protoplasts were mock or TCV-infected for 40 hrs and then analyzed by FISH using a Cy3-labelled probe complementary to bases 1210–1259 of the TCV genome. **d,** Quantification of mature miR-124 production from recombinant TCV was performed using the TaqMan miRNA assay on RNA from Fig. 4b. All samples were normalized to endogenous snoR66. Quantifications of each sample were performed in triplicate and error bars denote standard deviation from two biological replicates.

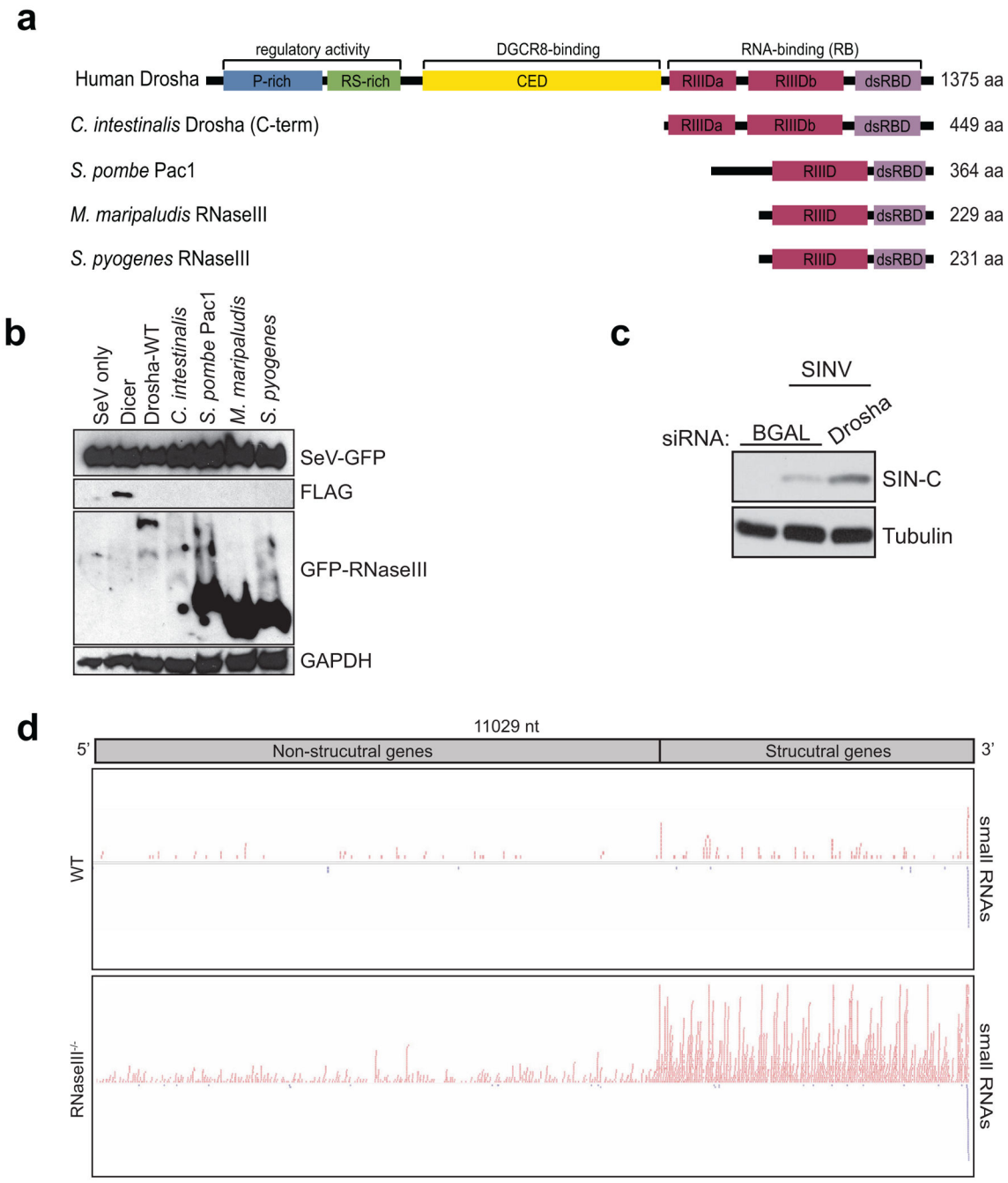

Extended Data Figure 7. The impact of diverse RNase III members on virus infection

a, Schematic depicting core domains of human Drosha, C-terminal region of *C. intestinalis* Drosha, or full length RNase IIIs of *S. pombe*, *M. maripaludis*, and *S. pyogenes*. Domains depicted include: Proline-rich, P-rich; arginine serine-rich, RS-rich; Conserved Central Domain, CED; RNAseIII domain (RIIID) and double stranded RNA binding domain (dsRBD). **b**, Western blots from BSR-T7 cells, co-transfected with the indicated RNase III-expression plasmids and SeV rescue plasmids encoding SeV-GFP genome, SeV-N, SeV-P, and SeV-L genes. RNase III expression was determined at 48 hpt and virus replication at 72

hpt. **c**, Western blot of DL1 cells treated with indicated dsRNA for 3 days and subsequently infected with SINV (MOI=1) for 96 hrs. **d**, 293T (WT) or RNaseIII$^{-/-}$ cells were infected with SINV for 24 hrs. Graphs depict the number of SINV reads mapping to indicated positions along the viral genomes from the small RNA deep sequencing performed in Extended Data Fig. 1b.

Supplementary Material

Refer to Web version on PubMed Central for supplementary material.

Acknowledgments

We wish to thank Drs. J.K. Lim (ISMMS) and A.A. Pletnev for Langat virus reagents, B. Lee (ISMMS) for Sendai virus reagents, R.W. Hardy (Indiana University) for Sindbis virus reagents, B.R. Cullen (Duke University) for NoDice cells, K.K. Conzelmann (Ludwig-Maximilians-University) for BSR-T7 cells, and B. Ramratnam (Brown University) for pEGFP-Drosha. rIFNB was provided by NIH's Biodefense and Emerging Infections Research Resources Repository (HuIFN-β,NR-3080). This material is based upon work supported in part by the Burroughs Wellcome Fund which provide support for both SC and BRT. SC is also supported by the National Institute of Allergy and Infectious Diseases (NIAID) (R01A1074951). JPL is supported by the DIM Malinf, Conseil Regional d'Ile-de-France. LCA is partially supported by the American Heart Association (15PRE24930012). AES is supported by National Science Foundation (MCB-1411836) and NIAID (R21AI117882). JM is supported by National Institute of General Medicine (F32 GM119235). BRT is also supported by NIAID (R01AI110575).

References

1. Koonin EV, Wolf YI, Nagasaki K, Dolja VV. The Big Bang of picorna-like virus evolution antedates the radiation of eukaryotic supergroups. Nat Rev Microbiol. 2008; 6:925–939. DOI: 10.1038/nrmicro2030 [PubMed: 18997823]
2. ten Oever BR. The Evolution of Antiviral Defense Systems. Cell Host Microbe. 2016; 19:142–149. DOI: 10.1016/j.chom.2016.01.006 [PubMed: 26867173]
3. ten Oever BR. RNA viruses and the host microRNA machinery. Nat Rev Microbiol. 2013; 11:169–180. DOI: 10.1038/nrmicro2971 [PubMed: 23411862]
4. Cerutti H, Casas-Mollano JA. On the origin and functions of RNA-mediated silencing: from protists to man. Curr Genet. 2006; 50:81–99. DOI: 10.1007/s00294-006-0078-x [PubMed: 16691418]
5. Obbard DJ, Jiggins FM, Halligan DL, Little TJ. Natural selection drives extremely rapid evolution in antiviral RNAi genes. Curr Biol. 2006; 16:580–585. DOI: 10.1016/j.cub.2006.01.065 [PubMed: 16546082]
6. Shapiro JS, Langlois RA, Pham AM, Tenoever BR. Evidence for a cytoplasmic microprocessor of pri-miRNAs. RNA. 2012; 18:1338–1346. DOI: 10.1261/rna.032268.112 [PubMed: 22635403]
7. Shapiro JS, Varble A, Pham AM, Tenoever BR. Noncanonical cytoplasmic processing of viral microRNAs. RNA. 2010; 16:2068–2074. DOI: 10.1261/rna.2303610 [PubMed: 20841420]
8. Rouha H, Thurner C, Mandl CW. Functional microRNA generated from a cytoplasmic RNA virus. Nucleic Acids Res. 2010; 38:8328–8337. DOI: 10.1093/nar/gkq681 [PubMed: 20705652]
9. Bogerd HP, Whisnant AW, Kennedy EM, Flores O, Cullen BR. Derivation and characterization of Dicer- and microRNA-deficient human cells. RNA. 2014; 20:923–937. DOI: 10.1261/rna.044545.114 [PubMed: 24757167]
10. Han J, et al. The Drosha-DGCR8 complex in primary microRNA processing. Genes Dev. 2004; 18:3016–3027. DOI: 10.1101/gad.1262504 [PubMed: 15574589]
11. Triboulet R, Chang HM, Lapierre RJ, Gregory RI. Post-transcriptional control of DGCR8 expression by the Microprocessor. RNA. 2009; 15:1005–1011. DOI: 10.1261/rna.1591709 [PubMed: 19383765]
12. Tang X, Zhang Y, Tucker L, Ramratnam B. Phosphorylation of the RNase III enzyme Drosha at Serine300 or Serine302 is required for its nuclear localization. Nucleic Acids Res. 2010; 38:6610–6619. DOI: 10.1093/nar/gkq547 [PubMed: 20554852]

13. Court DL, et al. RNase III: Genetics and function; structure and mechanism. Annu Rev Genet. 2013; 47:405–431. DOI: 10.1146/annurev-genet-110711-155618 [PubMed: 24274754]
14. Shirako Y, Strauss EG, Strauss JH. Modification of the 5′ terminus of Sindbis virus genomic RNA allows nsP4 RNA polymerases with nonaromatic amino acids at the N terminus to function in RNA replication. J Virol. 2003; 77:2301–2309. [PubMed: 12551967]
15. Tsetsarkin KA, Liu G, Shen K, Pletnev AG. Kissing-loop interaction between 5′ and 3′ ends of tick-borne Langat virus genome 'bridges the gap' between mosquito- and tick-borne flaviviruses in mechanisms of viral RNA cyclization: applications for virus attenuation and vaccine development. Nucleic Acids Res. 2016; 44:3330–3350. DOI: 10.1093/nar/gkw061 [PubMed: 26850640]
16. Bick MJ, et al. Expression of the zinc-finger antiviral protein inhibits alphavirus replication. J Virol. 2003; 77:11555–11562. [PubMed: 14557641]
17. Rupp JC, Jundt N, Hardy RW. Requirement for the amino-terminal domain of sindbis virus nsP4 during virus infection. J Virol. 2011; 85:3449–3460. DOI: 10.1128/JVI.02058-10 [PubMed: 21248049]
18. Moy RH, et al. Stem-loop recognition by DDX17 facilitates miRNA processing and antiviral defense. Cell. 2014; 158:764–777. DOI: 10.1016/j.cell.2014.06.023 [PubMed: 25126784]
19. Shapiro JS, et al. Drosha as an interferon-independent antiviral factor. Proc Natl Acad Sci U S A. 2014; 111:7108–7113. DOI: 10.1073/pnas.1319635111 [PubMed: 24778219]
20. Sabin LR, et al. Dicer-2 processes diverse viral RNA species. PLoS One. 2013; 8:e55458. [PubMed: 23424633]
21. Sarkar D, Desalle R, Fisher PB. Evolution of MDA-5/RIG-I-dependent innate immunity: independent evolution by domain grafting. Proc Natl Acad Sci U S A. 2008; 105:17040–17045. DOI: 10.1073/pnas.0804956105 [PubMed: 18971330]
22. Maillard PV, et al. Inactivation of the type I interferon pathway reveals long double-stranded RNA-mediated RNA interference in mammalian cells. EMBO J. 2016
23. Seo GJ, et al. Reciprocal inhibition between intracellular antiviral signaling and the RNAi machinery in mammalian cells. Cell Host Microbe. 2013; 14:435–445. DOI: 10.1016/j.chom.2013.09.002 [PubMed: 24075860]
24. Varble A, et al. An in vivo RNAi screening approach to identify host determinants of virus replication. Cell Host Microbe. 2013; 14:346–356. DOI: 10.1016/j.chom.2013.08.007 [PubMed: 24034620]
25. Cheng EH, Levine B, Boise LH, Thompson CB, Hardwick JM. Bax-independent inhibition of apoptosis by Bcl-XL. Nature. 1996; 379:554–556. DOI: 10.1038/379554a0 [PubMed: 8596636]
26. Zhang F, Simon AE. A novel procedure for the localization of viral RNAs in protoplasts and whole plants. Plant J. 2003; 35:665–673. [PubMed: 12940959]
27. Perez JT, et al. MicroRNA-mediated species-specific attenuation of influenza A virus. Nat Biotechnol. 2009; 27:572–576. DOI: 10.1038/nbt.1542 [PubMed: 19483680]
28. Cherry S, Perrimon N. Entry is a rate-limiting step for viral infection in a Drosophila melanogaster model of pathogenesis. Nat Immunol. 2004; 5:81–87. DOI: 10.1038/ni1019 [PubMed: 14691479]
29. Chong MM, Rasmussen JP, Rudensky AY, Littman DR. The RNAseIII enzyme Drosha is critical in T cells for preventing lethal inflammatory disease. J Exp Med. 2008; 205:2005–2017. DOI: 10.1084/jem.20081219 [PubMed: 18725527]
30. Ossovskaya V, Lim ST, Ota N, Schlaepfer DD, Ilic D. FAK nuclear export signal sequences. FEBS Lett. 2008; 582:2402–2406. DOI: 10.1016/j.febslet.2008.06.004 [PubMed: 18549812]
31. Pall GS, Hamilton AJ. Improved northern blot method for enhanced detection of small RNA. Nat Protoc. 2008; 3:1077–1084. DOI: 10.1038/nprot.2008.67 [PubMed: 18536652]
32. Robinson JT, et al. Integrative genomics viewer. Nat Biotechnol. 2011; 29:24–26. DOI: 10.1038/nbt.1754 [PubMed: 21221095]
33. Sedano CD, Sarnow P. Hepatitis C virus subverts liver-specific miR-122 to protect the viral genome from exoribonuclease Xrn2. Cell Host Microbe. 2014; 16:257–264. DOI: 10.1016/j.chom.2014.07.006 [PubMed: 25121753]
34. Manley JL. SELEX to identify protein-binding sites on RNA. Cold Spring Harb Protoc. 2013; 2013:156–163. DOI: 10.1101/pdb.prot072934 [PubMed: 23378656]

35. Rio DC. Electrophoretic mobility shift assays for RNA-protein complexes. Cold Spring Harb Protoc. 2014; 2014:435–440. DOI: 10.1101/pdb.prot080721 [PubMed: 24692495]

36. Lee Y, et al. The nuclear RNase III Drosha initiates microRNA processing. Nature. 2003; 425:415–419. DOI: 10.1038/nature01957 [PubMed: 14508493]

37. Hardy RW, Rice CM. Requirements at the 3′ end of the sindbis virus genome for efficient synthesis of minus-strand RNA. J Virol. 2005; 79:4630–4639. DOI: 10.1128/JVI.79.8.4630-4639.2005 [PubMed: 15795249]

38. McCormack JC, Simon AE. Callus cultures of Arabidopsis. Curr Protoc Microbiol. 2006; Chapter 16(Unit16D.11)

39. Shaffer SM, Wu MT, Levesque MJ, Raj A. Turbo FISH: a method for rapid single molecule RNA FISH. PLoS One. 2013; 8:e75120. [PubMed: 24066168]

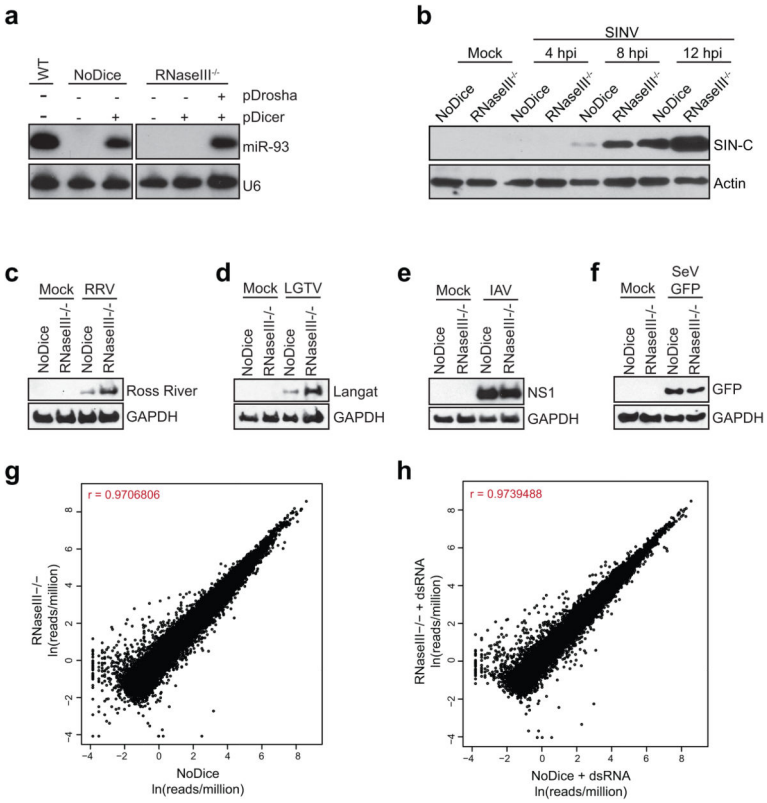

Figure 1. Drosha mediates miRNA-independent antiviral activity

a, Northern blot (NB) of RNA from NoDice and RNaseIII$^{-/-}$ cells reconstituted with indicated plasmids. Blots probed for miR-93 and U6. **b**, Western blot (WB) of whole cell extract from NoDice and RNaseIII$^{-/-}$ cells infected with SINV (MOI=0.01) at 4, 8, and 12 hpi. Blot probed for SINV Capsid (SIN-C) and pan-Actin (Actin). **c–f**, WBs of Ross River virus (MOI=0.1) (**c**), Langat virus (MOI=0.1) (**d**), Influenza virus (MOI=1) and (**e**), GFP-encoding Sendai virus (MOI=1) (**f**). Protein levels were assessed at 24 hpi using virus-specific or GFP antibodies as indicated. **g**, RNA-Seq correlation analyses of NoDice and RNaseIII$^{-/-}$ cells at baseline. **h**, As described in **g**, except cells were treated with dsRNA for 8 hrs. Graphs in g and h depict data from biological replicates.

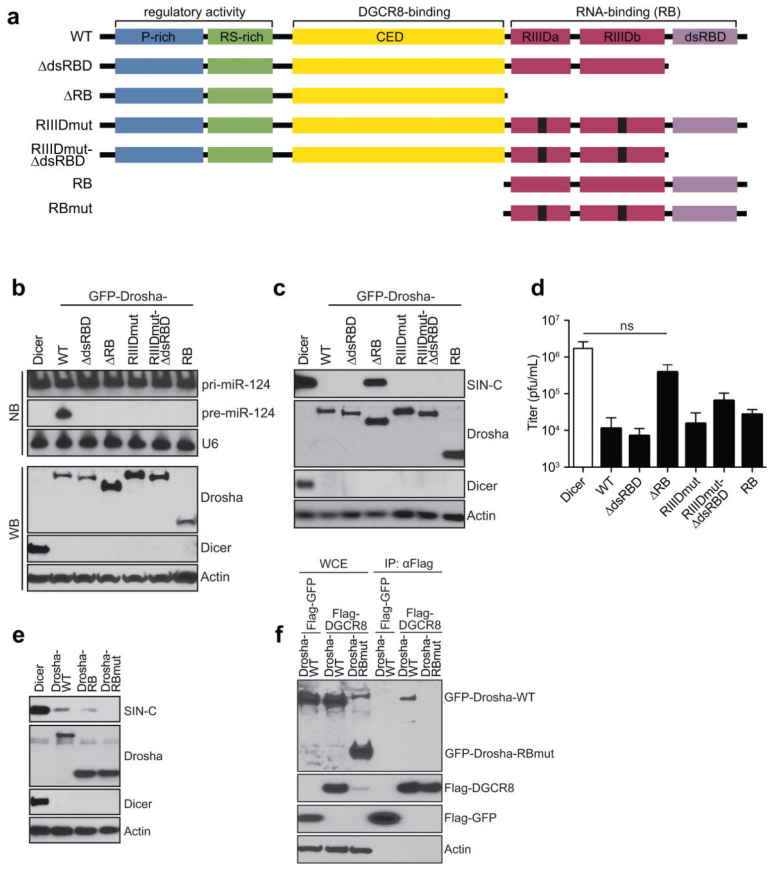

Figure 2. The RNA-binding domain of Drosha is essential for virus inhibition

a, Core domains and variants of Drosha including: Proline-rich, P-rich; arginine serine-rich, RS-rich; Conserved Central Domain, CED; RNAseIII domain (RIIID) and double-stranded RNA binding domain (dsRBD). Black boxes indicate point mutations (mut) **b,** NB and WB of RNaseIII$^{-/-}$ cells transfected with the indicated Drosha variants and cytoplasmic miR-124. WB depicts Drosha, Dicer, and pan-Actin. **c,** WB and **d,** titers from RNaseIII$^{-/-}$ cells expressing the indicated transcripts and SINV RNA 24 hpt. Graph denotes average titers obtained with error bars generated using standard deviation from three independent experiments. 'ns' denotes not significant, all other conditions had a p-value of <0.05. **e,** WB as described in **c** with Drosha RBmut. **f,** WB of input and Flag-immunoprecipitated (IP) fractions derived from 293T cells expressing indicated transcripts and Flag-DGCR8.

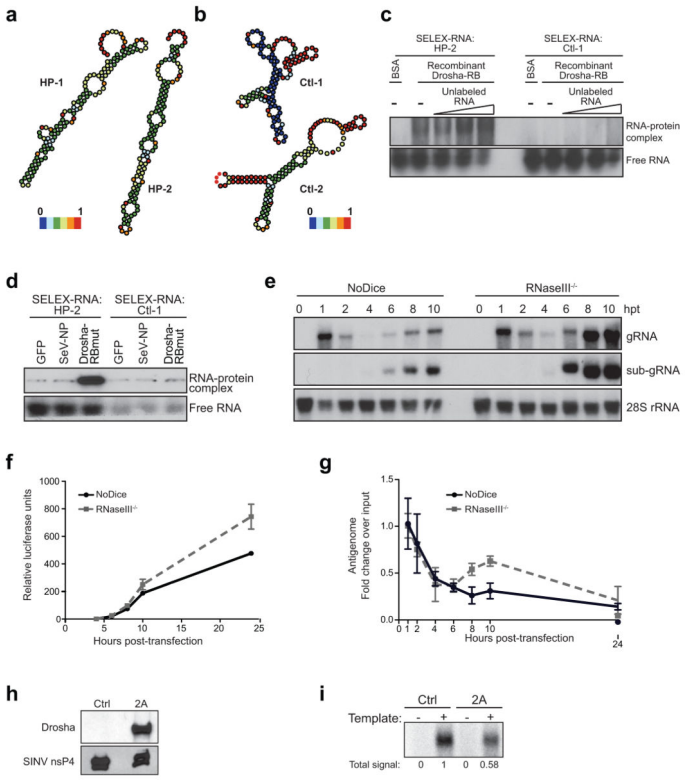

Figure 3. Cytoplasmic Drosha binds stem-loop structures in viral RNA to inhibit RdRp activity

a, RNA hairpins (HP-1/-2) enriched by Drosha-RBmut-based SELEX as predicted by RNAfold. **b,** same as **a,** using GFP as control (Ctl-1/02) bait. **c**, RNA-based EMSA of hairpins in **a,** and **b,** using recombinant Drosha-RB. **d**, EMSA as in **c,** performed with immunoprecipitated GFP, Sendai nucleoprotein (SeV-NP), or Drosha-RBmut. **e**, NB of RNA from NoDice and RNaseIII$^{-/-}$ transfected a SINV-based replicon denoting genomic (g) and subgenomic (sub-g) SINV RNA. **f–g,** luciferase (**f**) and antigenome expression (**g**) of replicon as described in **e.** Data is representative of independent experiments where each condition was done in triplicate. Error bars denote standard deviation. **h,** WB of cytoplasmic membrane fractions from control or Drosha-2A cells expressing SINV replicase-components. **i**, *in vitro* minus strand RNA synthesis assay utilizing membrane fractions from **h**.

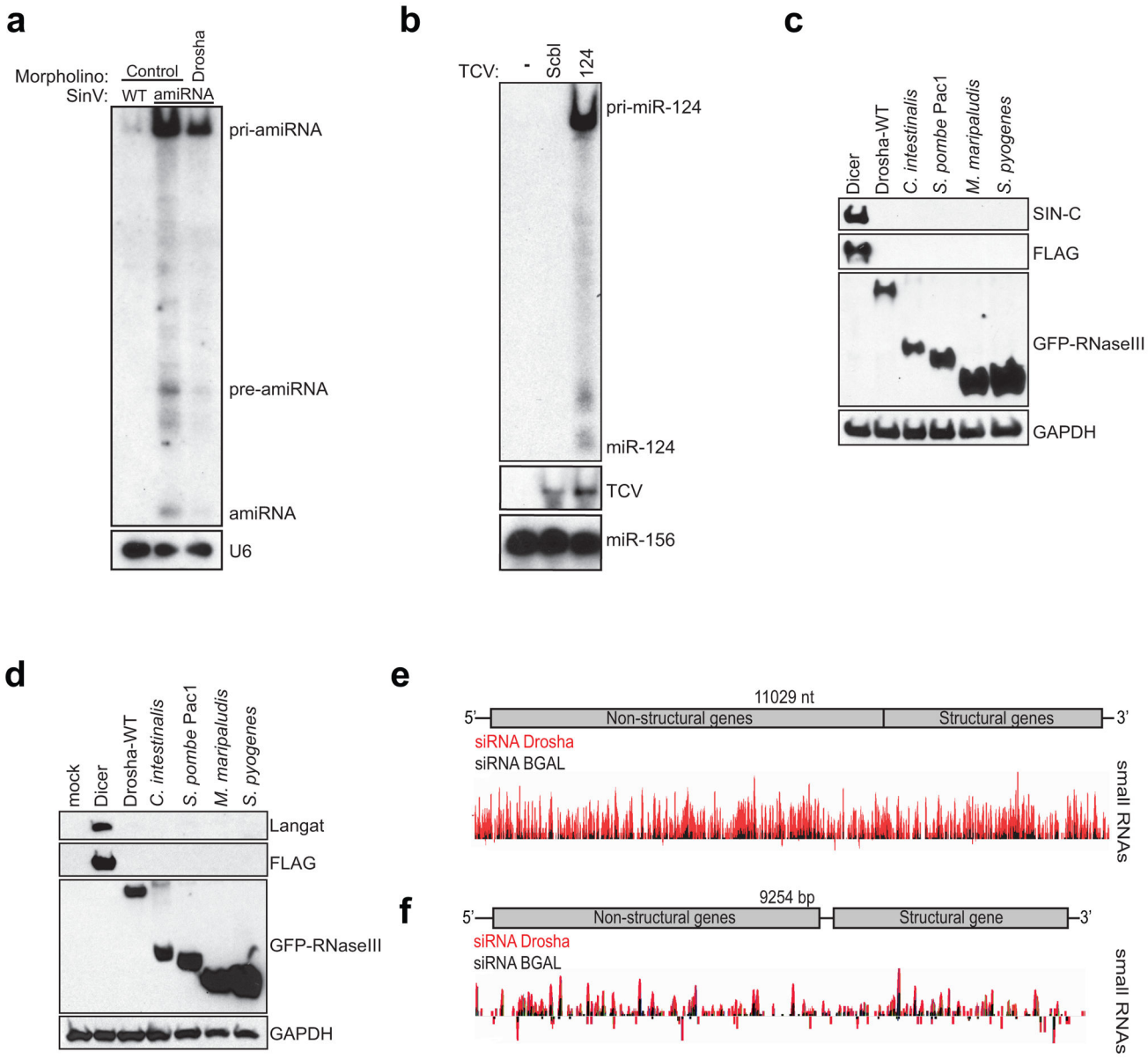

Figure 4. RNase III inhibition of virus replication is highly conserved

a, NB of RNA from zebrafish embryos treated with indicated morpholinos, and inoculated 2 days later with wild type SINV (WT) or a strain encoding an artificial miRNA (amiRNA). Blot depicts amiRNA and U6 at 40hrs post infection **b**, NB of RNA from *Arabidopsis thaliana* protoplasts treated with a *Turnip crinkle virus* (TCV) containing a scrambled sequence (Scbl) or miR-124 (124). **c and d**, WB from RNaseIII$^{-/-}$ cells, co-transfected with the indicated plasmids and either *in vitro* transcribed SINV gRNA or Langat virus rescue plasmid. **e and f,** Small RNA-Seq of DL1 cells treated with indicated dsRNA for 3 days and subsequently infected with SINV (MOI=1) (**e**) or DCV (MOI=7) (**f**). Graphs depict the number of reads mapping to indicated positions along the viral genomes.